Microgravity-Science and Technology (2018) 30:155–163
https://doi.org/10.1007/s12217-017-9584-3

ORIGINAL ARTICLE

Extreme Adiabatic Expansion in Micro-gravity: Modeling for the Cold Atomic Laboratory

C. A. Sackett[1] · T. C. Lam[1] · J. C. Stickney[2] · J. H. Burke[3]

Received: 13 June 2017 / Accepted: 5 December 2017 / Published online: 15 December 2017

Abstract
The upcoming Cold Atom Laboratory mission for the International Space Station will allow the investigation of ultracold gases in a microgravity environment. Cold atomic samples will be produced using evaporative cooling in a magnetic chip trap. We investigate here the possibility to release atoms from the trap via adiabatic expansion. We discuss both general considerations and a detailed model of the planned apparatus. We find that it should be possible to reduce the mean trap confinement frequency to about 0.2 Hz, which will correspond to a three-dimensional sample temperature of about 150 pK and a mean atom velocity of 0.1 mm/s.

Keywords Ultracold atoms · Cold atom laboratory · Adiabatic cooling

Introduction

The Cold Atom Laboratory (CAL) is an ultra-cold atom apparatus being developed for the International Space Station by NASA and the Jet Propulsion Laboratory (http://coldatomlab.jpl.nasa.gov). The goal of the apparatus is to conduct cold-atom experiments in microgravity, enabling the study of atomic gases free from the effects of confinement forces. Previous efforts in this area have used ground-based drop towers, achieving microgravity conditions for about 10 s duration but with experimental repetition rates of only a few per day (Müntinga and et al. 2013; Kulas and et al. 2017). Atomic fountain experiments can achieve durations of about 1 s at a much higher repetition rate (Kovachy et al. 2015). Recently, a sounding rocket experiment achieved 300 s of microgravity conditions (Lachmann and et al. 2017). The CAL experiment will have the advantage of essentially unlimited microgravity time with a fast repetition rate, although the duration of a particular experiment will still be limited to about 10 s by the vacuum conditions in the apparatus.

A significant motivation for this effort is the opportunity to produce and investigate a gas of nearly stationary atoms in free space. This could be useful for sensor applications like atom interferometry (Cronin et al. 2009; Sorrentino and et al. 2010) and equivalence principle tests (Lämmerzahl 2003; Rudolph and et al. 2011). The atoms might serve as a proof mass in navigation and force-sensing experiments comparable to Gravity Probe B (Everitt and et al. 2011) and MICROSCOPE (Touboul et al. 2012). With long interrogation times in a perturbation-free environment, the atoms could be a source for high-precision spectroscopy and atomic clocks (Lemonde 1998; Laurent et al. 2015).

Microgravity offers obvious benefits for working with a near-stationary atomic sample. However, to take advantage of from this it is necessary to first prepare the atoms with low velocities relative to the apparatus. In thermal equilibrium, this corresponds to a very low temperature. Optimally the atoms should form a Bose-Einstein condensate, in which a macroscopic fraction of the atoms occupy the ground state of the confining potential (Dalfovo et al. 1999; Müntinga and et al. 2013). Ideally, the energy of the ground state is limited only by Heisenberg's uncertainty principle, such that the energy increases as the atoms are more tightly confined.

✉ C. A. Sackett
sackett@virginia.edu

[1] Physics Department, University of Virginia, Charlottesville, VA 22904, USA

[2] Space Dynamics Laboratory, North Logan, UT 84341, USA

[3] US Air Force Research Laboratory, Space Vehicles Directorate, Kirtland AFB, NM 87117, USA

A tightly-confining trap is necessary for producing a condensate using evaporative cooling (Ketterle et al. 1998), and if such a trap is turned off quickly the resulting sample will have a relatively large velocity spread. This effect is exacerbated by the fact that atoms in a condensate generally interact via an effectively repulsive potential, which leads to even larger velocities upon release (Dalfovo et al. 1999).

A solution is to controllably expand the sample to a large volume where the atoms can be brought nearly to rest with negligible constraints from interactions or the uncertainty principle. At the same time, it is often necessary to position the center of the sample at a desired location, where for instance the atoms can be accessed by laser beams for further experimentation.

There are at least two ways to achieve these results. In one method, known as delta-kick collimation (DKC), the atom trap is quickly turned off, causing the atom cloud to rapidly expand, but later the trap is briefly pulsed back on with the correct time and strength to bring the expanded atoms nearly to rest (Ammann and Christensen 1997; Aoki et al. 2006; Müntinga and et al. 2013). A second method is adiabatic expansion. Here the atom trap is slowly weakened and the atom cloud expands quasi-reversibly as the confinement is reduced (Kastberg et al. 1995; Leanhardt et al. 2003). Once the cloud is a suitable size, the residual weak trap can be quickly turned off. In the limit of large expansion in an ideal harmonic trap, both of these methods are theoretically equivalent and produce the same final momentum spread for a given sample size. The choice between them is therefore based on practical considerations. Most significantly, the DKC method requires very precise control of the trapping fields and it can be degraded by any anharmonicity of the trap. Adiabatic expansion is insensitive to the details of the trap but because the potential is made very weak, the cooling is easily spoiled by uncontrolled background fields. In addition, adiabatic cooling requires significantly more time, which can be a constraint given the finite vacuum lifetime.

Experimental study of either technique is difficult on the ground because of the strong effect of gravity. Nonetheless considerable work on DKC has been performed by the QUANTUS group using the Bremen drop tower to achieve microgravity conditions for several seconds (Müntinga and et al. 2013). They were able achieve sample energies equivalent to temperatures below 1 nK. Alternatively, in a tall atomic fountain Kovachy *et al.* used DKC to achieve effective two-dimensional temperatures of about 50 pK (Kovachy et al. 2015). Adiabatic expansion has not been studied as extensively, since it requires more free-fall time. However, experiments with magnetically trapped atoms have obtained temperatures as low as 500 pK (Leanhardt et al. 2003). It is planned for both approaches to be investigated and compared in the CAL apparatus.

We focus in this paper on the adiabatic cooling technique. We first address some general factors regarding the method, including the production of a weak trap and the dynamics of adiabaticity. We then discuss a detailed model of the CAL apparatus and a proposed cooling trajectory for use with it. We find that with the expected level of background magnetic field and trapped-atom lifetime, it should be possible to reach three-dimensional effective temperatures of about 150 pK.

Analysis of an Ideal Trap

We first consider the general question of producing a weak trap using an apparatus like that of CAL. This will provide useful context for more specific numerical simulations. The CAL apparatus uses a magnetic chip trap. In general a magnetic trap confines atoms using a magnetic field, via the Zeeman interaction (Pérez-Ríos and Sanz 2013). An atom in the trap experiences a potential energy $U = -\mu B$, where B is the field magnitude $|\mathbf{B}|$ and μ is the effective magnetic moment $\mu = -g_F m_F \mu_B$, for an atom in hyperfine state F with magnetic quantum number m_F. Here g_F is the Landé factor and μ_B is the Bohr magneton. Atoms with $\mu < 0$ are trapped at a minimum of B.

In a chip trap, the atoms are held near a surface using a field produced by wires lithographically patterned onto the surface (Fortagh and Zimmermann 2007). In particular, the CAL apparatus provides a 'Z-trap,' which can be idealized as the geometry shown in Fig. 1. A current I flows through the wire, and a uniform external bias field has components B_{0x} and B_{0y}. A positive bias B_{0y} will cancel the field from the short wire segment at some height z above the chip, leading to a field minimum and thus an atom trap near that point.

The trap field $\mathbf{B}$ at any location (x, y, z) can be readily calculated using the Biot-Savart law. For instance, at $x = y = 0$ the field from the wire is

$$\mathbf{B}(z) = -\frac{\mu_0 I}{2\pi}\left(\frac{z}{z^2+a^2}\hat{x} + \frac{a}{z\sqrt{z^2+a^2}}\hat{y}\right). \quad (1)$$

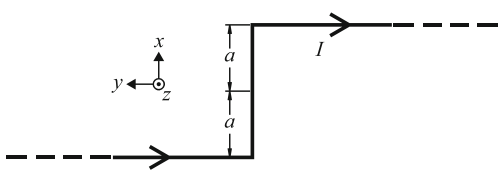

Fig. 1 Geometry of the Z-wire trap. The thick black line represents the wire on the atom chip, carrying current I in the direction indicated. The dashed lines indicate where, ideally, the straight wire segments extend to infinity. The axes indicate the coordinate directions, with the origin in the plane of the chip at the center of the short segment. In addition to the magnetic field from the wire, the trap uses a uniform bias field pointing in the xy-plane

When added to the uniform bias fields, this gives the total field experienced by the atoms.

Near the field minimum, the potential energy can be approximated as that of a harmonic oscillator. The corresponding oscillation frequencies can be determined as

$$\omega_q = \left(-\frac{\mu}{m}\lambda_q\right)^{1/2} \tag{2}$$

where m is the atomic mass and the $\{\lambda_q\}$ are the eigenvalues of the Hessian matrix $H_{ij} = \partial^2 B/\partial x_i \partial x_j$. A useful measure of the strength of the trap is the geometrical average of the three frequencies $\bar{\omega} = (\omega_1\omega_2\omega_3)^{1/3}$ (Dalfovo et al. 1999). For adiabatic expansion, we wish to create a trap with $\bar{\omega}$ as small as possible.

An obvious way to make an arbitrarily weak trap is to start with a strong trap and then uniformly reduce the current and bias fields. However, in practice the apparatus is located within a background field $\delta\mathbf{B}$ which may not be accurately known or stable. If the trapping fields are very small, the contribution of $\delta\mathbf{B}$ can be significant and can alter the trap or make it unconfining. We therefore impose a constraint that the field at the center of the trap, B_0, must remain large compared to $\delta B = |\delta\mathbf{B}|$. This makes the problem more complicated. To facilitate analysis, we can first calculate the B_{0x} and B_{0y} bias fields need to produce a trap minimum at position z_0 and with a net minimum field B_0. This yields

$$B_{0x} = \frac{B_0}{\sqrt{1+\beta^2}} + \frac{\mu_0 I}{2\pi}\frac{z_0}{z_0^2+a^2} \tag{3}$$

and

$$B_{0y} = \frac{\beta B_0}{\sqrt{1+\beta^2}} + \frac{\mu_0 I}{2\pi}\frac{a}{z_0\sqrt{z_0^2+a^2}}, \tag{4}$$

where the geometrical parameter β is given by

$$\beta = \frac{z_0^2\left(a^2-z_0^2\right)}{a\left(2z_0^2+a^2\right)\sqrt{z_0^2+a^2}}. \tag{5}$$

With z_0 and B_0 fixed, the only remaining variable in the trapping potential is the current, which can be expressed in the dimensionless form $\kappa \equiv \mu_0 I/(2\pi a B_0)$. We can therefore solve for the trap frequencies as a function of κ alone. At some current, one of the ω_q approaches zero, and thus $\bar{\omega} \to 0$. However, in this condition the atoms again become susceptible to small forces from the background field. Therefore, we instead solve for the current where the smallest of the trap frequencies, $\omega_{\min}$, reaches a desired value. This gives the weakest usable trap at a given position and minimum field. Figure 2 shows the z_0 dependence of $\bar{f} = \bar{\omega}/2\pi$, for a few different values of B_0 and $f_{\min} = \omega_{\min}/2\pi$. In each case, there is an optimum trap position that provides the lowest $\bar{\omega}$. As z_0 becomes small, $\bar{\omega}$ increases as the confinement along the x direction becomes very weak relative to that along y and z. As z_0 becomes large, a similar

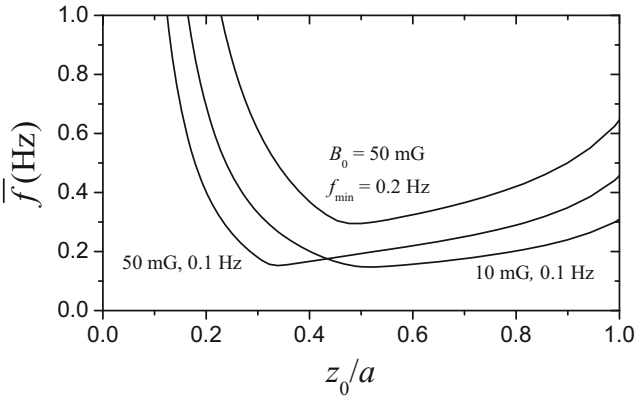

Fig. 2 Minimum achievable trapping frequency for an ideal Z trap, as a function of trap position z_0 and for various values of the trap minimum field B_0 and lowest permissible oscillation frequency in any direction, $f_{\min}$. Here $\bar{f}$ is the geometric mean of oscillation frequencies along the three principle directions of the trap, and a characterizes the size of the Z-trap wire

effect occurs because at $z \approx 1.20a$, there is a saddle point in the field such that one trap frequency approaches zero, regardless of the current. This, incidentally, represents a limit to the distance the atoms can be adiabatically displaced from the chip.

Figure 3 shows the dependence of the trapping parameters on the $f_{\min}$ criterion. Plot 3(a) shows how $\bar{f}$ increases with $f_{\min}$. In general, a large minimum field does not appear to be a hindrance for obtaining a weak trap. Plot 3(b) shows the resulting trap positions, with larger B_0 generally allowing a weak trap closer to the chip and smaller B_0 allowing a larger displacement.

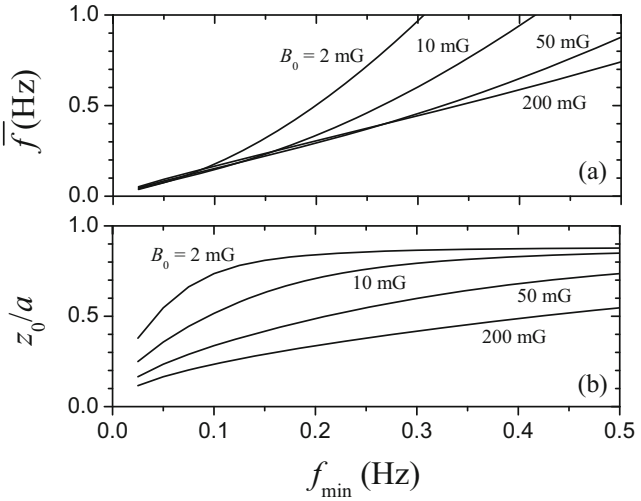

Fig. 3 Trap dependence on the minimum confinement strength requirement. Here the trap position z_0 was chosen to give the minimum possible average frequency $\bar{f}$ at each specified minimum frequency $f_{\min}$. The different traces show the results for different trap minimum field B_0

The minimum usable value for $f_{\min}$ is expected to be set by the background field tolerance. In the limit $\delta B \ll B_0$, the total magnetic field $\mathbf{B}_{\text{tot}} = \mathbf{B} + \delta\mathbf{B}$ can be expanded to first order to obtain

$$|\mathbf{B}_{\text{tot}}| \approx B + \frac{\mathbf{B} \cdot \delta\mathbf{B}}{B}, \tag{6}$$

so in this limit the component of $\delta\mathbf{B}$ along the trapping field contributes directly to the potential. A gradient $\delta B'$ in this component will cause the trap position to shift by a distance on the order of

$$\xi \approx \frac{\mu}{m} \frac{\delta B'}{{\omega_{\min}}^2}, \tag{7}$$

assuming that $\bar{\omega}$ is not very different from $\omega_{\min}$. In addition, a curvature $\delta B''$ will shift the trap frequencies by an amount of order

$$\delta\omega \approx \frac{\mu}{2m\omega_{\min}} \delta B''. \tag{8}$$

The exact size of these shifts will depend on the relation between the trap principle axes and the bias field direction, which varies with z_0. Roughly, however, these conditions relate $f_{\min}$ to the tolerances in $\delta\mathbf{B}$.

The CAL experiment will have both Rb and K atoms available. We focus for now on Rb, and discuss the implication for K atoms in the conclusion. The CAL chip has $a = 0.26$ cm, and the background field is expected to have $\delta B < 1$ mG, $\delta B' < 10$ mG/cm, and $\delta B'' < 10$ mG/cm^2. This suggests that a minimum field $B_0 > 10$ mG is sufficient. The curvature tolerance is consistent with a trap frequency as low as 0.1 Hz for Rb atoms. These parameters would allow a mean frequency $\bar{f}$ of 0.15 Hz, at a distance of about 1 mm from the chip.

The gradient tolerance is a more significant constraint. If the induced displacement ξ is comparable to z_0, then the trap confinement will be affected. Further, the atoms might be displaced away from laser beams needed for subsequent experiments. To avoid this, we might require $\xi < 1$ mm and therefore $f_{\min} > 0.4$ Hz. This in turn yields $\bar{f} \approx 0.5$ Hz, which is considerably larger than the curvature constraint. However, it is expected that the background gradient will be mostly static, since it primarily derives from imperfect shielding of magnetic components within the apparatus. As will be discussed in Section 3, it should be possible to compensate for a static gradient. If these can be used to reduce $\delta B'$ by a factor of 10, then $f_{\min} \rightarrow 0.13$ Hz and $\bar{f} \approx 0.2$ Hz could be achieved.

It is interesting to consider the nominal temperature achievable for a given expanded trap. If the expansion is adiabatic, then the condensate fraction N_0/N remains a useful measure of temperature via

$$T = T_c \left(1 - \frac{N_0}{N}\right)^{1/3}, \tag{9}$$

and $k_B T_c = 0.94\hbar\bar{\omega}N^{1/3}$ (Dalfovo et al. 1999). For $N = 10^4$ atoms and a typical observable condensate fraction $N_0/N = 0.8$, this yields an expanded temperature of about 100 pK at $\bar{f} = 0.2$ Hz. At $\bar{f} = 0.5$ Hz, a temperature of 250 pK would be accessible.

Adiabaticity

Although extreme expansion requires the ability to produce a weak trap, it is also important to maintain adiabaticity during the expansion. Certainly, if the trap is relaxed slowly enough, then the atoms will adiabatically follow. However, the lifetime of the atoms in the trap is limited, so it is beneficial to perform the expansion as rapidly as possible, given an acceptable amount of non-adiabatic excitation. The anticipated $1/e$ lifetime of atoms in the CAL apparatus is about 10 s.

We use a simple model consisting of classical particles in a harmonic potential. An initial concern is the treatment of interactions between the particles. There are three issues to consider. First, in a tight trap the density can be so high that the mean free path is short compared to the size of the atom cloud. In this case the interactions can have significant impact during a rapid expansion. The initial stages of the trap expansion are likely to be in this regime, for trap frequencies of a few hundred Hz or higher. However, for such large trap frequencies the expansion rate can be made much slower than ω without requiring excessive time, and in that case we expect the expansion to be generically adiabatic.

A second concern is when the collision rate becomes slow compare to the lifetime of the system. This occurs at frequencies on the order of 10 Hz. In this regime it is not clear that the system will be in equilibrium with a well-defined temperature. We can instead determine the average energy of the gas, and relate that to the hypothetical temperature that would be achieved if the system came to equilibrium. This is a common convention used, for instance, in Müntinga and et al. (2013) and Kovachy et al. (2015).

Finally, the atoms in a Bose-Einstein condensate generate a repulsive mean-field potential, characterized by the chemical potential μ. This potential effects the dynamics of both the condensed and non-condensed atoms in a non-trivial way. To our knowledge, the impact of this effect on slow expansion of an atomic gas has not been theoretically addressed, and it will be an interesting feature to investigate with CAL. However, the effect of interactions on the dynamics is not expected to be dramatic. For instance, the collective excitation frequencies typically differ by only a modest amount from the non-interacting case (Dalfovo et al. 1999).

As a first approximation, we therefore ignore the effects of interactions and consider the expansion of an ideal gas. Our goal is to determine how slowly the trap must be expanded to keep the non-adiabatic effects small, and as long as they are small it is not necessary to characterize them very accurately. Furthermore, our results suggest that excitation of the center-of-mass motion is the most sensitive type of nonadiabaticity. In a harmonic trap this separates from the relative motion, so interactions have negligible effect on the center of mass. We thus expect our results for that degree of freedom to be reasonably accurate.

Since the harmonic potential is also separable by dimensions, we consider a one-dimensional model with trapping potential

$$V(z,t) = \frac{1}{2} m\omega(t)^2 \left[z - z_0(t)\right]^2 \tag{10}$$

where $\omega(t)$ is the oscillation frequency and $z_0(t)$ the trap position, both functions of time. We numerically solve the classical equation of motion in this potential, as the frequency is reduced from ω_i to ω_f and the trap is displaced by a distance δz. We modeled a 200-fold reduction in trap frequency, representing the final stage of a cooling experiment.

Presumably there is an optimum form of time-dependence for $\omega(t)$, given a fixed duration $T_{\rm ramp}$ for the expansion. Indeed, DKC could itself be considered a particular form of expansion time-dependence. We here focus on smooth and continuous expansions, for which we explored various models. We found good performance using a scaled tanh ramp,

$$\omega(t) = \left(\frac{\omega_i + \omega_f}{2}\right) + \left(\frac{\omega_f - \omega_i}{2}\right) \frac{\tanh(5u)}{\tanh(5)}, \tag{11}$$

with $u(t) = [2(t/T_{\rm ramp})^{1/4} - 1]$ for time t running from 0 to $T_{\rm ramp}$. The inset of Fig. 4 shows a graph of $\omega(t)$.

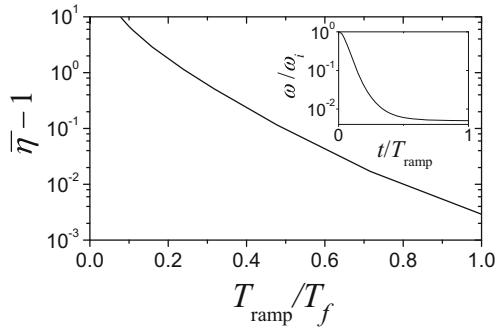

Fig. 4 Adiabaticity of expansion as a function of ramp time. Here $\bar{\eta}$ is the ratio of the energy after the expansion to the value obtained in the perfectly adiabatic case, averaged over the phase of the initial motion. $T_{\rm ramp}$ is the total time taken for the expansion, and T_f is the oscillation period in the final trap. In this case the trap center is not displaced while the trap frequency is reduced by a factor of 200. The inset shows the trap frequency as a function of time t during the ramp

We consider first non-adiabatic excitations coming from parametric excitation of the particle motion, keeping z_0 constant. We model this by providing the particle with an initial excitation energy E_i. We then calculate the trajectory and determine the final energy E_f after the expansion. This determines an adiabaticity parameter

$$\eta = \frac{E_f \omega_i}{E_i \omega_f}. \tag{12}$$

Perfectly adiabatic motion would yield $\eta = 1$. Generally the actual value of η depends on the phase of the initial particle motion, relative to the start of the ramp. In an ensemble of many atoms, all different phases would occur, so we average over the initial phase to calculate an effective value $\bar{\eta}$. To a reasonable approximation, $\bar{\eta}$ can be used to characterize the temperature increase of a thermal sample relative to perfect adiabaticity.

Figure 4 shows the results obtained for $\bar{\eta}$, with $T_{\rm ramp}$ expressed in terms of the final trap period $T_f = 2\pi/\omega_f$. It can be seen that the adiabaticity requirement is fairly forgiving, with a ramp time of $0.5T_f$ yielding an average energy increase of about 10% above perfect adiabaticity.

We next consider the case where the trap center is displaced. We assume here that the shift $\delta z = z_0(T_{\rm ramp}) - z_0(0)$ is due to uncontrolled background field gradients so that its direction and magnitude are not well known. To the extent that the shift is known, the expansion time-dependence can often be manipulated to help compensate for it (*cf.* Section 3). In light of Eq. 7, we allow z_0 to vary as

$$z_0(t) = \delta z \, \frac{\omega(t)^{-2} - \omega_i^{-2}}{\omega_f^{-2} - \omega_i^{-2}}, \tag{13}$$

using the tanh ramp of Eq. 11 for $\omega(t)$. Here we start with the particle at rest at $z = 0$ and calculate the energy after the ramp.

The natural energy scale for the motional excitation is $E_\delta = m\omega_f^2 \delta z^2/2$. Our results are shown in Fig. 5. Here again a ramp time of roughly the final period is sufficient to be mostly adiabatic, but in this case E_δ could be rather large if the trap is displaced by a sizable amount. For instance, if $\omega_f = 2\pi \times 0.2$ Hz then Rb atoms would have $E_\delta/\delta z^2 = 8.3$ nK/mm^2. Obtaining $E_f < 100$ pK for a trap displacement $\delta z = 1$ mm would thus require a ramp time of about $2T_f$, or 10 s. This is marginally consistent with the expected vacuum lifetime of the apparatus.

Numerical Model

The idealized model of Section 3 leaves out significant aspects of the actual trap. For instance, the input and output wires in Fig. 1 actually continue straight for only a finite distance, and the bias fields are not actually uniform. An

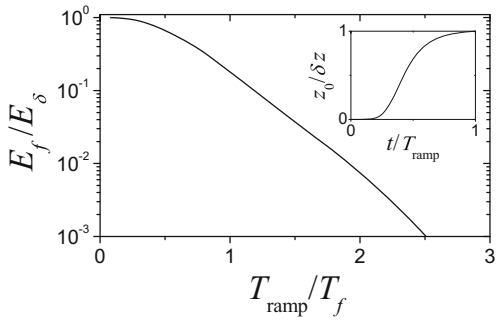

Fig. 5 Energy gained when the trap position shifts during the expansion. The inset shows how the trap center z_0 moves as a function of time t. Here E_f is the final energy of the particle, and $E_\delta = m\omega_f^2 \delta z^2/2$, where trap center shifts by an amount δz as the confinement frequency is relaxed as in Fig. 4 to a final frequency ω_f. The total time of the expansion is $T_{\rm ramp}$, and the final period is $T_f = 2\pi/\omega_f$

illustration of the CAL chip is shown in Fig. 6. Typically, when the atoms are trapped close to the chip these non-idealities have little impact. However, in a weak trap far from the chip they can be expected to be important.

We modeled both the chip and the bias field coils in detail. We used an in-house general purpose trap modeling program, named ARAMOT. It consists of a Biot-Savart

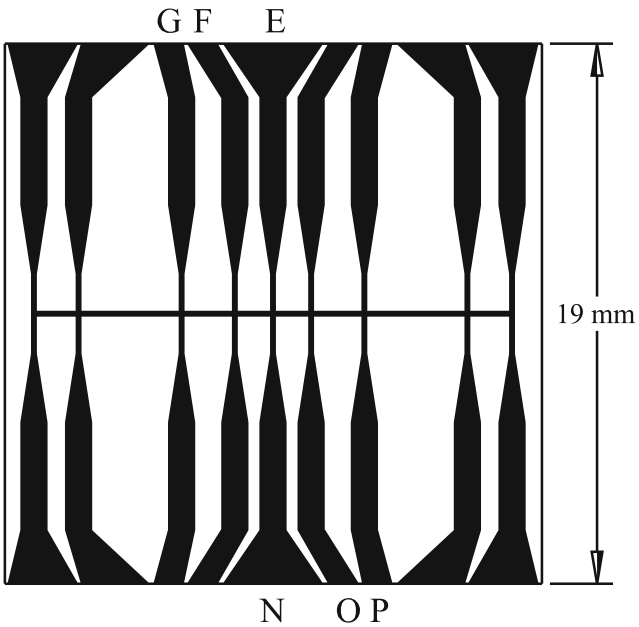

Fig. 6 Scale drawing of the CAL atom chip. The black traces are current-carrying elements, with driver connections at the chip edges. The horizontal strip serves as a common bus line. Two independent current drivers are available. One is connected to elements E and N, and is used to produce a tight trap for evaporative cooling and also for gradient compensation during adiabatic expansion. The second driver can be switched between circuits F-O and G-P. The former produces a tight Z-trap for evaporation, while the later makes a weaker trap more useful for expansion

calculator with a convenient graphical interface for setting up the wire geometries. Since the cold atoms are held relatively far from the chip, we treated the chip traces as thin wires. We included the full current paths through the chip, and 1-cm-long wires leading to the chip. Detailed information on the lead-wire geometry is not available, but doubling the length of the leads had little effect on the trap.

We used ARAMOT to determine the magnetic trap potential, find the trap minimum, and calculate the atom oscillation frequencies. We sought a trap configuration with a minimum located 1 mm from the chip, which provides a reasonable expansion volume and room for a laser beam in subsequent experiments. Guided by the results from Section 3, we used a trap minimum field of 20 mG. We obtained a trap roughly consistent with the ideal results, with trap frequencies of 0.12 Hz, 0.31 Hz, and 0.43 Hz for a mean frequency $\bar{f} = 0.25$ Hz. This is consistent with the expected usable $f_{\rm min}$ value, and the approximately symmetric trap provides a low $\bar{f}$ for a given $f_{\rm min}$. The trap uses a current of 2 mA in the G-P trace of Fig. 6, along with bias fields $B_{0x} \approx 20$ mG and $B_{0y} \approx 2$ mG.

As previously noted, this trap should permit temperatures of about 150 pK. This corresponds to a velocity of 0.15 mm/s, and would thus provide a useful atomic sample for a free-fall experiment of several seconds duration.

We explored the process of transferring atoms from a tight trap near the chip to the final weak trap. The initial trap used a Z-trap current running from connection F to connection O in Fig. 6, with the smallest possible size a. In addition, a small current flowed through the 'dimple' wire from E to N, which increases the confinement in the x direction. The final configuration used only a current through the larger Z wire from F to P. Unfortunately, larger-Z configurations are unavailable due to constraints in the driver design.

We developed a sequence of five ramps controlling the various chip currents and bias fields. Each of the ramps was linear in a scaled time variable u defined by

$$\tan(\theta u) = \left(\frac{t}{T}\right)^{\gamma} \tan\theta \tag{14}$$

where here t is measured from the start of the ramp, T is the duration of the ramp, and γ and θ are constants chosen to minimize motional excitation and ensure a smooth transition between successive ramps. This form was chosen as the most convenient and best performing of several scaling variations. The ramp parameters are shown in Table 1, and the results are shown in Fig. 7. Over the course of the 5-s sequence, the mean trap frequency is reduced by a factor of 4400.

We tested the behavior of atoms in the trap using a classical three dimensional model similar to that of Section 3. We calculated the trajectory of an atom starting at

Table 1 Trap drive parameters for adiabatic expansion

Stage	Duration	I_{GP}	I_{FO}	I_{EN}	B_x	B_y	γ	$\pi/2-\theta$
1	0.2 s	0 A	3.2 A	0.12 A	0.6 G	25 G	0.8	1.5
2	0.8	0	2.0	0	0.6	10	0.9	0.03
3	0.6	2.0	0	0	60 mG	3.18	0.5	0.5
4	0.7	0.5	0	0	60	0.79	1.0	0.3
5	2.7	50 mA	0	0	60	75 mG	0.65	0.02
6	–	2	0	0	20	2 mG	–	–

The expansion uses five ramps, starting from the parameters listed as stage 1. The listed duration shows the time taken to ramp to the next stage, where stage 6 is the final configuration achieved after 5 s total. The current values refer to the circuit connections of Fig. 6. During each ramp, all the current and field parameters are changed together using a nonlinear scaling function set by γ and θ, as described in the text

rest for the time-varying trap position and frequency values determined by ARAMOT. We find that an atom starting at rest ends up with an energy of 70 pK in the final trap. In a three-dimensional harmonic trap this corresponds to a temperature of 23 pK, which is comfortably lower than the estimated temperature we hope to achieve.

It should be noted that the atom motion during the ramp is not truly adiabatic. In particular, during the first part of the ramp where the trap center is moved, the atoms acquire some excitation which is later mostly removed. This is illustrated in Fig. 8, where for perfect adiabaticity $E/\hbar\bar{\omega}$ would remain constant. The initial gain and later loss of energy was found to be robust, and did not depend significantly on the duration or time dependence of the initial ramp, nor on small shifts in the bias fields. We therefore expect that the same behavior would occur in the experiment, resulting in acceptably low motional excitation.

Finally, we used the detailed model to investigate compensation of background field gradients. The apparatus has one pair of coils (along x) that can be driven differentially to provide gradient cancellation. In general, however, three independent gradient fields are required to cancel an arbitrary background. A second compensation can be obtained from the E-N wire on the chip (Fig. 6). This changes the bias field along x and produces a gradient similar to $x\hat{z} - z\hat{x}$. A small change in B_x has little effect, but can be compensated by the bias coils if necessary. For a third control, a bias field along z can be applied. This does not directly provide a significant gradient, but it causes the location of the trap minimum to shift in the y direction. The trap fields themselves can then provide the third gradient component at the desired trap location.

We tested these methods in the simulation by applying a small current to each element, and observing how the trap location shifted. From that and the known trap frequencies, the effective gradient could then be determined, as in Eq. 7. The results are shown in Table 2. Here the magnitude and direction of the gradient refers to the vector $\nabla(\mathbf{B}_i \cdot \mathbf{B}_0/B_0)$, where $\mathbf{B}_i$ is the field from the specified source and $\mathbf{B}_0$ is the trap minimum field. The fact that the three sources produce gradients in independent directions means they can indeed

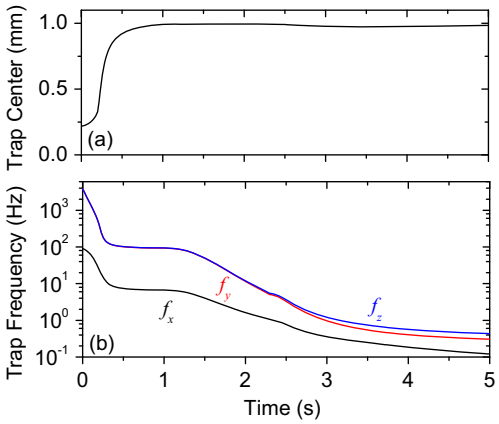

Fig. 7 (Color online) Transition from a tight trap for evaporative cooling to a weak trap. The upper graph (**a**) shows the motion of the trap center as the distance from the atom chip, z_0, is increased to approximately 1 mm. The lower graph (**b**) shows the three trap frequencies f_x, f_y, and f_z as the trap strength is decreased

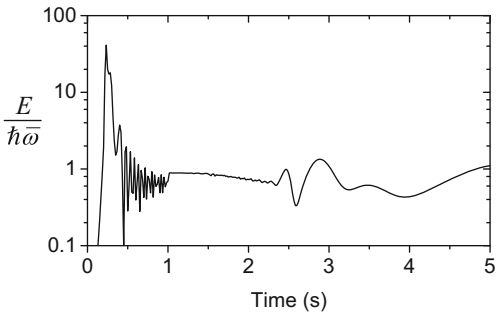

Fig. 8 Adiabaticity of ramp. The vertical axis shows the energy E of a classical atom in the trap, starting initially at rest. The energy is scaled by the mean confinement frequency of the trap $\bar{\omega}$ and Planck's constant. In an adiabatic expansion, $E/\hbar\bar{\omega}$ would remain constant. The peak in the early part of the plot shows energy being acquired as the trap center moves, and then mostly removed as the trap center comes back to rest. This excitation energy is mainly in the z coordinate, which is the direction the trap is moving

Table 2 Numerical results for gradient sources

Gradient source	Magnitude	$\hat{x}$	$\hat{y}$	$\hat{z}$
X coils	17 (G/cm)/A	−1	0	0
E-N wire	23	0	0	1
Z coils	50	−0.96	0.24	0.14

The source indicates the field element, as discussed in the text. The magnitude gives the gradient in the component of the field parallel to the bias field of the trap per unit of current. The $\hat{x}$, $\hat{y}$, and $\hat{z}$ entries show the direction of the gradient of the relevant field component, as a unit vector

be used to compensate for arbitrary small environmental fields δB. This compensation will be adjusted *in situ* once the apparatus has been installed.

Conclusion

We have considered the problem of adiabatically releasing atoms from a magnetic trap in a microgravity environment. We hope to have illustrated both some general considerations and a specific plan for the upcoming CAL experiment. Our results suggest that a 5-s to 10-s expansion time should be sufficient to release a sample at a temperature equivalent of about 150 pK, including energy in the center-of-mass motion. Achieving lower temperatures by this method would likely require both better control of background magnetic fields and longer vacuum lifetimes for expansion.

For clarity, we summarize here the "temperature budget" used in our simple approach. We suppose that the apparatus initially produces $N = 10^4$ atoms in a tight trap, with condensate fraction $N_0/N = 0.8$. If this sample were reversibly expanded into a final trap with $\bar{f} = 0.25$ Hz, the final temperature would be 140 pK. The chemical potential of the condensate would be 28 pK, corresponding to a condensate energy of 8 pK after the trap is turned off (Dalfovo et al. 1999). Our modelling in Section 3 suggests that both of these values would be increased by about 10% due to parametric excitations, for a temperature of 155 pK and a condensate energy per atom of 9 pK. Non-adiabatic excitation of the center-of-mass motion would then contribute 70 pK to the total energy due to the calculated ramp (Section 3), and about 100 pK due to uncompensated background gradient shifts (Section 3). Both of these are divided by three to give an equivalent temperature increase, and since we expect the motions to be uncorrelated, we add them in quadrature to yield a final temperature estimate of 160 pK. The total condensate energy per atom would be 40 pK per coordinate, almost entirely in the center-of-mass motion.

It is not expected that the CAL apparatus will be able to produce a Bose condensate for K atoms, but rather a thermal sample close to the condensation temperature. In a harmonic trap, the oscillation frequency for K is about 1.5 times larger than for Rb, so the expanded trap will give a mean frequency of $\bar{f} = 0.37$ Hz for K atoms. At 10^4 atoms this yields a transition temperature of 360 pK. The higher oscillation frequency means that the K atoms are less sensitive than Rb to non-adiabatic effects, so we expect that a temperature on this order should be achievable. A dual-species experiment should yield a similar temperature for both species, given that the atoms are at least initially in thermal equilibrium. The higher temperature for Rb here reflects the fact that evaporative cooling will be less efficient so the atoms start out warmer than expected for a pure Rb sample.

It remains a question how the adiabatic (or quasi-adiabatic) approach will compare to DKC techniques. Certainly the delta-kick method is faster, and since the applied fields are always large, it is less constrained by the presence of small background fields. However, the cooling effectiveness of DKC is likely to be limited by anharmonicity in the collimating potential. Also, a complex series of kicks will be required to move the atoms away from the chip and then bring them to rest at the correct position. The effectiveness in practice will depend on how accurately the pulses can be implemented, which will need to be explored. All these challenges for DKC are increased if it is desired to cool both Rb and K atoms simultaneously.

It may be that this should not be considered an either/or question, but instead the optimal practice could be a combination of adiabatic and DKC stages. Alternatively, classical control techniques might be used to find a rapid but not impulsive series of trap changes which ultimately bring the atoms nearly to rest (Feddema et al. 1997).

In any case, as microgravity experiments are developed, the need for an effective method for motional state preparation will become more important. We hope that the work here stimulates further discussion of the problem.

Acknowledgements This work was supported by the US National Aeronautics and Space Administration under contract number 1502012, and also by the US Air Force Research Laboratory. We are grateful to Rob Thompson of JPL for providing information about the CAL trap design, and thank both him and Eddie Moan for comments on the manuscript.

References

Ammann, H., Christensen, N.: Phys. Rev. Lett. **78**, 2088 (1997)
Aoki, T., Kato, T., Tanami, Y., Nakamatsu, H.: Phys. Rev. A **73**, 063603 (2006)
Cronin, A.D., Schmiedmayer, J., Pritchard, D.E.: Rev. Mod. Phys. **81**, 1051 (2009)

Dalfovo, F., Giorgini, S., Pitaevskii, L., Stringari, S.: Rev. Mod. Phys. **71**, 463 (1999)
Everitt, C.W.F., et al.: Phys. Rev. Lett. **106**, 221101 (2011)
Feddema, J.T., Dohrmann, C.R., Parker, G.G., Robinett, R.D., Romero, V.J., Schmitt, D.J.: IEEE Control. Syst. **17**, 29 (1997)
Fortagh, J., Zimmermann, C.: Rev. Mod. Phys. **79**, 235 (2007)
Kastberg, A., Phillips, W.D., Rolston, S.L., Spreeuw, R.J.C., Jessen, P.S.: Phys. Rev. Lett. **74**, 1543 (1995)
Ketterle, W., Durfee, D.S., Stamper-kurn, D.M.: In: Proceedings of the international school of physics enrico fermi, course CXL Bose-Einstein condensation in atomic gases, North Holland, p. 67 (1998)
Kovachy, T., Hogan, J.M., Sugarbaker, A., Dickerson, S.M., Donnelly, C.A.: Phys. Rev. Lett. **114**, 143004 (2015)
Kulas, S., et al.: Microgravity Sci. Technol. **29**, 37 (2017)
Lachmann, M., et al.: Bull. Am. Phys. Soc. **62**, J7.4 (2017)
Lämmerzahl, C.: In: Giulini, D., Kiefer, C., Lämmerzahl, C. (eds.) Quantum gravity: from theory to experimental search, p. 367. Springer, Berlin (2003)
Laurent, P., Massonnet, D., Cacciapuoti, L., Salomon, C.: C. R. Phys. **16**, 540 (2015)
Leanhardt, A.E., Shin, Y., Chikkatur, A.P., Kielpinski, D., Ketterle, W., Pritchard, D.E.: Phys. Rev. Lett. **90**, 100404 (2003)
Lemonde, P.: Microgravity Sci. Technol. **11**, 85 (1998)
Müntinga, H., et al.: Phys. Rev. Lett. **110**, 093602 (2013)
Pérez-Ríos, J., Sanz, A.S.: Am. J. Phys. **81**, 836 (2013)
Rudolph, J., et al.: Microgravity Sci. Technol. **23**, 287 (2011)
Sorrentino, F., et al.: Microgravity Sci. Technol. **22**, 551 (2010)
Touboul, P., Métris, G., Lebat, V., Robert, A.: Class. Quant. Gravity **29**, 184010 (2012)